THE JOURNAL OF PHYSICAL CHEMISTRY A
A JOURNAL OF THE AMERICAN CHEMICAL SOCIETY

pubs.acs.org/JPCA

Article

Electrochemical Ring-Opening and -Closing of a Spiropyran

Jorn D. Steen, Daniël R. Duijnstee, Andy S. Sardjan, Jacopo Martinelli, Luuk Kortekaas, Denis Jacquemin,* and Wesley R. Browne*

Cite This: *J. Phys. Chem. A* 2021, 125, 3355−3361

Read Online

ACCESS | Metrics & More | Article Recommendations | Supporting Information

ABSTRACT: The bistability of molecular switches is an essential characteristic in their use as functional components in molecular-based devices and machines. For photoswitches, light-driven switching between two stable states proceeds via short-lived changes of the bond order in electronically excited states. Here, bistable switching of a ditertbutyl-substituted spiropyran photoswitch is instead demonstrated by oxidation and subsequent reduction in an overall four-state cycle. The spiropyran structure chosen has reduced sensitivity to the effect of secondary electrochemical processes such as H^+ production and provides transient access to a decreased thermal *Z*−*E* isomerization barrier in the one electron oxidized state, akin to that achieved in the corresponding photochemical path. Thus, we show that the energy needed for switching spiropyrans to the merocyanine form on demand, typically delivered by a photon, can instead be provided electrochemically. This opens up further opportunities for the utilization of spiropyrans in electrically controlled applications and devices.

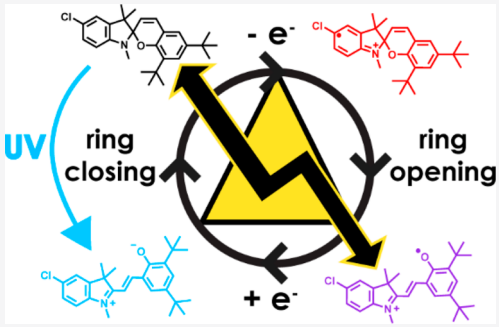

INTRODUCTION

The bistability of molecular switches is central to their application in organic electronics and functional (smart) materials. Molecular photoswitches, for which light is used to toggle the molecular structure and hence molecular properties, have dominated the field of molecular switching for over a half century. As an alternative, or even complementary, switching pathway that opens up further opportunities, electrochemical switching has been investigated in a range of photochromes, e.g., stilbenes,[1,2] thioindigos,[3,4] fulgides,[5] azobenzenes,[6−8] overcrowded alkenes,[9,10] diarylethenes,[11−18] and, notably, imidazole dimer switches developed recently by Abe et al.[19] The challenge, however, in electrochemical switching of photochromes is to replicate fully the process driven by a photon using a redox cycle.

The spiropyran family of compounds shows chromic response, in addition to light, to a wide range of external stimuli.[20−22] Chromism can be triggered by external redox units, e.g., by oxidation of a ferrocene[23] or polyoxometalate moiety[24,25] or by oxidation or reduction of an ancillary carboxamidine moiety.[26] Among them, electrochemical input has been shown to cause spontaneous ring-opening of spiropyrans,[27−29] such as in the oxidative ring-opening of indolinooxazolidines[30,31] and the reductive ring-opening of nitro-substituted spiropyrans by Fujishima et al. and later Hartl et al.[32,33]

Switching between spiropyran and merocyanine forms electrochemically without the involvement of ancillary groups is synthetically advantageous. However, the oxidation of simple spiropyrans results in carbon−carbon bond formation via the indolino unit yielding dimers and releasing protons (Figure 1).[34,35]

Blocking of the para position of the indoline unit, as in a methyl-substituted spiropyran (**MeNSP**), disables dimerization, and the oxidation to the spiropyran radical cation becomes reversible (Figure 1). Electrochemical oxidation in these cases can, however, indirectly trigger spontaneous ring-opening through the protons generated at the electrode by protonation-driven ring-opening to the merocyanine *Z*-**MCH**$^+$.[36,37]

Computational studies indicate that ring-opening in the oxidized state can occur upon photoexcitation,[36] and hence, when electrochemical dimerization is avoided, formation of the spiropyran radical cation can facilitate ring-opening to the merocyanine form. Indeed, direct oxidative ring-opening of a spiropyran was recently shown by Kubo et al., where the stabilization of the phenoxyl radical was driven by the aromatization of the acridine substituent.[38] Subsequent reduction, however, recovered the spiro compound rather than the open zwitterionic form.

Here, we show that a ditertbutyl-substituted spiropyran, in which a chloro substituent prevents oxidative aryl-aryl coupling (**tbSP**, Scheme 1), has a sufficiently low oxidation potential to

Received: February 7, 2021
Revised: March 14, 2021
Published: April 16, 2021

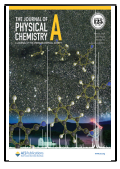

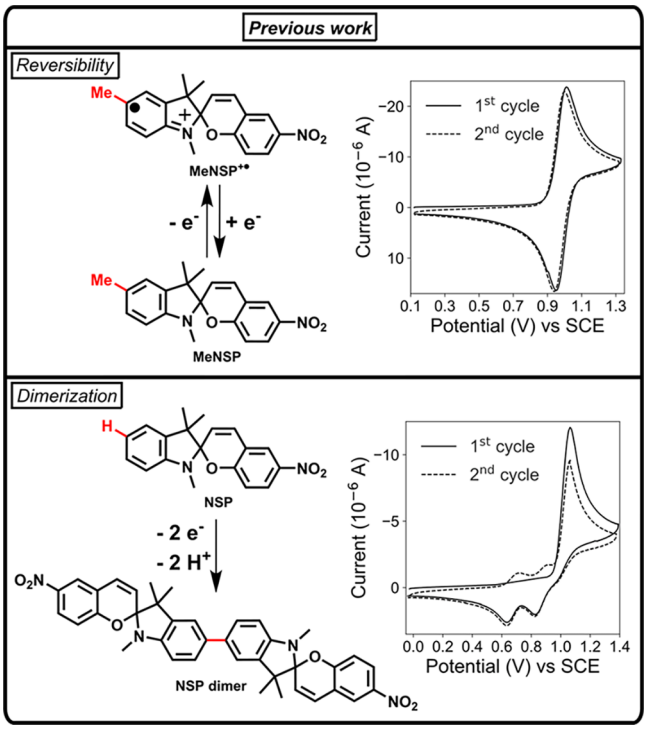

Figure 1. Redox chemistry of a nonsubstituted and a methyl-substituted nitrospiropyran. *Adapted in part from Browne et al.,[35] with permission from The Royal Society of Chemistry.

Scheme 1. Redox Chemistry of the Ditertbutyl-Spiropyran Reported Here. tbSP = Ditertbutyl-Spiropyran; tbMC = Ditertbutyl-Merocyanine

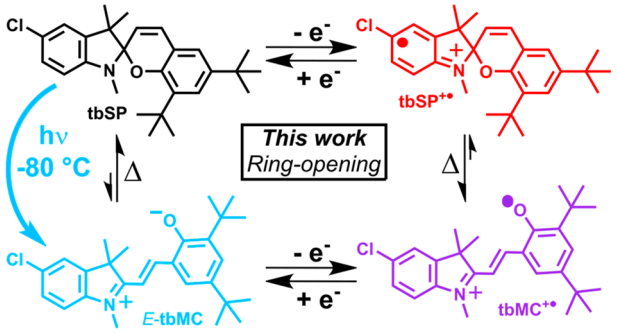

avoid competing acidochromism during electrochemical oxidation. The reversal in the relative stability of the spiropyran and merocyanine forms in the oxidized state is observed along with a low barrier to subsequent *Z*−*E* isomerization. The resulting thermally reversible electrocatalytic ring-opening of the spiropyran provides a new approach to bistable switching of spiropyrans.

METHODS

All chemicals for electrochemical and spectroscopic measurements and for the synthesis of **tbSP** were purchased from Sigma-Aldrich or TCI and were used without further purification. NMR spectra were obtained on a Bruker 400 spectrometer. Chemical shifts (δ) are reported in parts per million (ppm) with respect to tetramethylsilane and referenced to the residual solvent (CHD_2CN), and coupling constants are reported in hertz. Multiplicities are denoted as s = singlet, d = doublet, and m = multiplet. Electrospray ionization mass spectrometry was recorded on an LTQ Orbitrap XL spectrometer. Electron paramagnetic resonance (EPR) spectroscopy (X-band, 9.5 GHz) was performed on a Bruker EMX Nano spectrometer in liquid nitrogen at 77 K. Samples were flash frozen in a capillary tube in liquid nitrogen after generation of the desired species (monitored by UV−vis absorption spectroscopy). Fitting of EPR spectra was performed using EasySpin.[39] UV−vis absorption spectra at room temperature were recorded on an Analytik Jena Specord 600 spectrometer, and spectra at lower temperatures were recorded on an Agilent Technologies Cary 8454 spectrometer in a Unisoku CoolSpek USP-203-B cryostat. Irradiation at 340, 365, and 455 nm was provided by Thorlabs LEDs M340L4 (53 mW), M365LP1-C5 (435 mW), and M455L3-C5 (400 mW), respectively. Electrochemical measurements were performed on a model 604E or 760B electrochemical analyzer (CH Instruments). Typical analyte concentrations were 1.0 mM in acetonitrile (≥99.9%) or butyronitrile (≥99%) containing 0.1 M tetrabutylammonium hexafluorophosphate ($TBAPF_6$), and the electrodes employed were, unless stated otherwise, a 3 mm diameter Teflon-shrouded glassy carbon working electrode (CH Instruments), a Pt wire auxiliary electrode, and an Ag/AgCl wire reference electrode. Cyclic voltammetry at lower temperatures was carried out, at −84 °C, using a liquid nitrogen/ethyl acetate bath in a V-shaped tube, or, at −80 °C after irradiation, using a Unisoku temperature control cell in a 1 cm pathlength quartz cuvette. UV−vis absorption spectroelectrochemistry at room temperature was carried out using an optically transparent thin layer electrode cell, which consists of platinum mesh working and auxiliary electrodes, and an Ag/AgCl wire reference electrode in a liquid IR cell modified with quartz windows. Preparative oxidation and reduction experiments (bulk electrolysis) at lower temperatures were carried out in a Unisoku temperature control cell using a 2 mm pathlength quartz cuvette equipped with a Pt mesh working electrode, a Pt wire counter electrode, and an Ag/AgCl reference electrode.

RESULTS AND DISCUSSION

tbSP was prepared following the standard Fischer base synthetic procedure (see the Supporting Information) and characterized by ^{1}H NMR spectroscopy and high-resolution mass spectrometry.

Photo- and Acidochromism. As is the case with nonsubstituted spiropyrans,[22,40] **tbSP** does not show significant photochromism in solution at room temperature due to rapid thermal reversion of the merocyanine form to the spiropyran form. At −80 °C, UV irradiation generates the characteristic absorbance of a zwitterionic *E*-merocyanine (*E*-**tbMC**), with a distinctive vibrational structure that is more pronounced in solvents of lower polarity (Figure S1, vide infra). As with other spiropyrans, **tbSP** exhibits acidochromism.[37] Specifically, addition of near stoichiometric amounts of strong acids, e.g., CF_3SO_3H, results in protonation-driven ring-opening to the protonated *Z*-merocyanine isomer (*Z*-**tbMCH**$^+$), which undergoes both thermal and (reversible) photochemical conversion to the *E*-isomer (*E*-**tbMCH**$^+$). This change is manifested in a bathochromic shift of the UV−vis absorption band (Figures 2, S2, and S3). Addition of a base at room temperature to either form results in complete recovery of the original spectrum of **tbSP**, while at −40 °C intermediate formation of the deprotonated *E*-merocyanine (*E*-**tbMC**) is observed.

https://doi.org/10.1021/acs.jpca.1c01142
J. Phys. Chem. A 2021, 125, 3355−3361

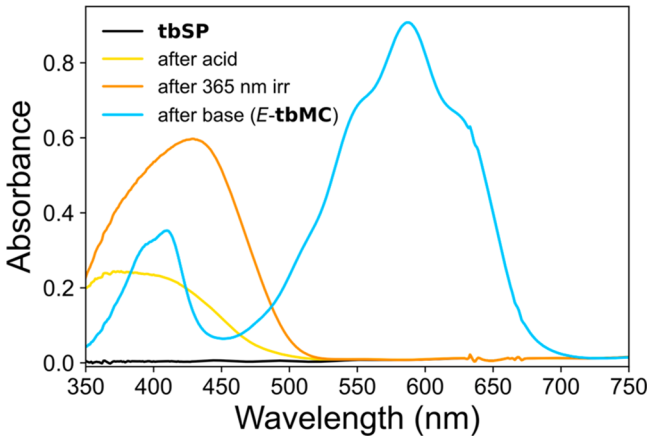

Figure 2. UV−vis absorption spectra of **tbSP** (45 μM) in acetonitrile at −40 °C (black) after addition of 2.5 equiv of CF_3SO_3H (yellow), subsequent irradiation with 365 nm (orange), and deprotonation with 25 equiv of NaOAc to yield *E*-**tbMC** (blue).

Cyclic Voltammetry. The cyclic voltammogram of **tbSP** at 0.1 V s^{-1} shows an irreversible oxidation at $E_{1/2}$ = 1.0 V vs Ag/AgCl and a subsequent irreversible reduction at $E_{1/2}$ = 0.45 V vs Ag/AgCl (Figures 3 and S4). At higher scan rates, both the

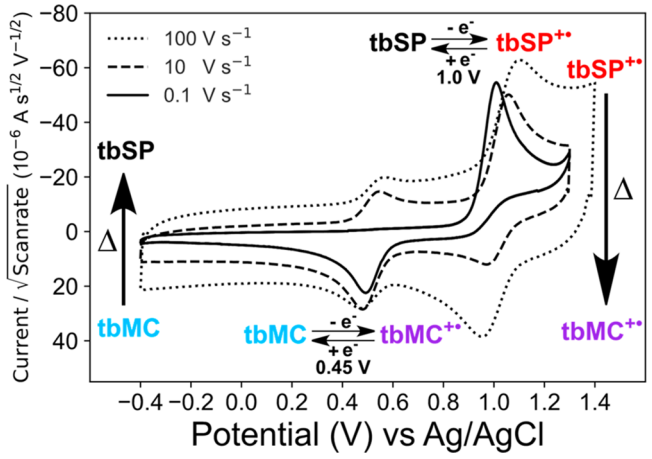

Figure 3. Cyclic voltammetry (2nd cycles shown only) of **tbSP** (1 mM) in acetonitrile (0.1 M $TBAPF_6$) at 20 °C at 0.1 (solid), 10 (dashed), and 100 V s^{-1} (dotted). The corresponding redox and chemical reactions are indicated. The 2nd cycles are shown for clarity to show also the reversibility of the redox process at 0.45 V. The 1st cycle in each case is identical except that the forward process at 0.45 V is absent (since the species responsible is not yet generated, see the Supporting Information).

redox wave at 1.0 V and the redox wave of the product at 0.45 V are electrochemically reversible ($E_{p,a} - E_{p,c}$ is ca. 70 mV). Note that the 2nd cycles are depicted, instead of the 1st, due to the appearance of the oxidation wave at 0.45 V only after the recording of an initial cycle. At −84 °C, the homogeneous reaction that follows oxidation of **tbSP** at 1.0 V is evidently inhibited as the chemical reversibility of the oxidation increases at 0.1 V s^{-1} (Figure S5). Thus, it seems that oxidation of the spiropyran to its radical cation **tbSP**$^{+\bullet}$ at 1.0 V, though electrochemically reversible, is followed by a chemically irreversible change to the open form radical cation **tbMC**$^{+\bullet}$. The **tbMC**$^{+\bullet}$ then undergoes an electrochemically reversible reduction to its neutral form **tbMC** (at 0.45 V) followed by thermal reversion to **tbSP** to complete the redox cycle (Scheme 1).

Density Functional Theory. DFT calculations (see the Supporting Information for computational details) are in good qualitative agreement with our proposed kinetic model and predict that, in the neutral state, ring-opening is uphill, while in the oxidized state, the process is downhill with a barrier of 6.0 kcal mol^{-1} for the breaking of the C−O bond and 15.8 kcal mol^{-1} for the *Z*−*E* isomerization (Figure 4). This low *Z*−*E*

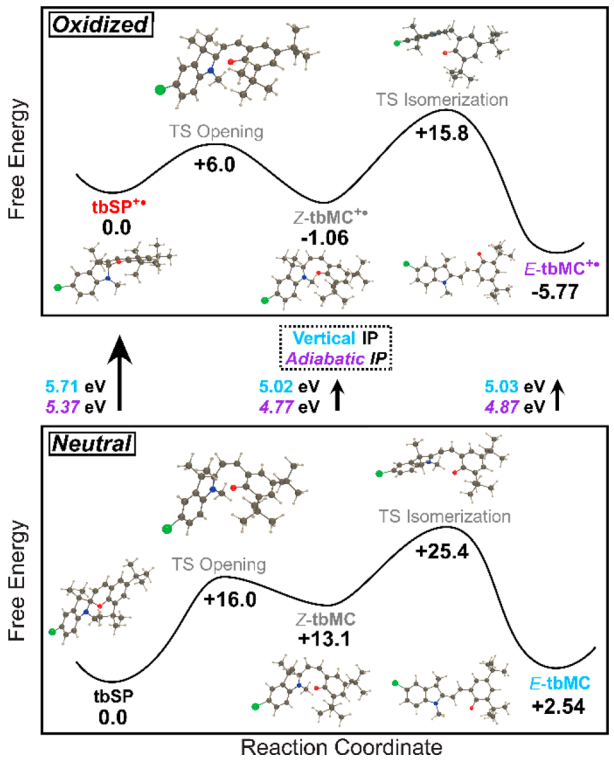

Figure 4. Reaction coordinate diagrams of **tbSP** ring-opening in neutral (bottom) and oxidized (top) states including each corresponding ionization potential (IP). The depicted mechanism describes a simplified model since there are multiple isomers of both *Z*- and *E*-open forms (see the Supporting Information). Relative free energies are given in kcal mol^{-1} taking the SP isomer as the reference for both structures.

isomerization barrier indicates that the *E*-**tbMC** species is obtained upon subsequent reduction. The total energy barrier for **tbSP**$^{+\bullet}$ ring-opening estimated from cyclic voltammetry by simulation is 15.4 kcal mol^{-1}, corresponding to a lifetime of approximately 50 ms (see the Supporting Information), which matches the value obtained by DFT calculations. In addition, the difference in computed adiabatic ionization energies for **tbSP** and *E*-**tbMC** of 0.50 eV (Figure 4) is also in good agreement with the experimentally observed difference in redox potential of 0.55 V between the two species (Figure 3).

The DFT calculations support that the merocyanine isomer *Z*-**tbMC** plays a role in the mechanism of ring-opening. Indeed, breaking the C_{spiro}−O bond yields *Z*-**tbMC** that is a true minimum (stable isomer) according to the calculation. In the neutral state, *Z*-**tbMC** is close in energy to the opening/closing transition state (TS opening), so that it is a transient species under experimental conditions. In contrast, the energy of *Z*-**tbMC**$^{+\bullet}$ is calculated to be lower than that of **tbSP**$^{+\bullet}$ and it should have a longer lifetime experimentally. Nevertheless,

https://doi.org/10.1021/acs.jpca.1c01142
J. Phys. Chem. A 2021, 125, 3355−3361

the *E*-isomer is substantially lower in energy with a rather small isomerization barrier (vide supra), and hence, its rapid formation upon oxidation of **tbSP** is expected even at low temperature. It should be noted that the *Z*- and *E*-isomers are in fact a manifold of isomers (see the Supporting Information);[22] however, the energy difference between these isomers is small and only the lowest energy conformers are presented in Figure 4. The low barriers for each step raise a question as to the detailed pathway for the electrochemical processes as rapid equilibria prior or after electron transfer steps will lead to essentially identical cyclic voltammograms.

Electrochemistry of Photochemically Generated *E*-Merocyanine. The redox chemistry of **tbMC** was investigated by making use of its initial photochemical generation from **tbSP** at −80 °C (with an absorbance of 0.9 at 590 nm and hence a concentration of 0.05 mM) followed by a cyclic voltammogram within a potential window of 0.0−0.7 V vs Ag/AgCl (Figures 5 and S6). Indeed, the observed reversible

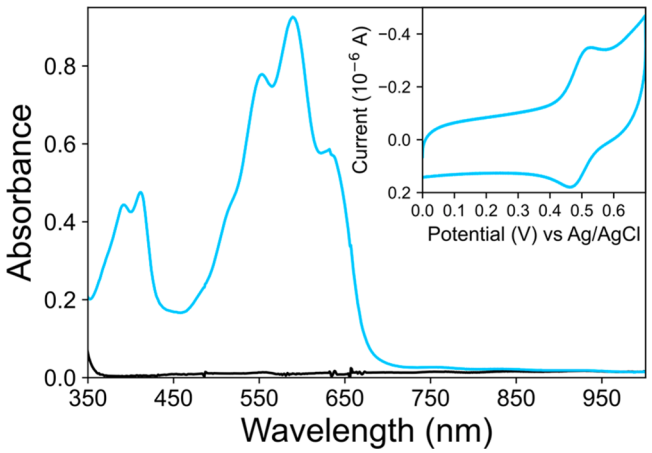

Figure 5. UV−vis absorption spectra of **tbSP** (2 mM) in butyronitrile (0.1 M $TBAPF_6$) at −80 °C before (black) and after irradiation at 340 nm to form **tbMC** (blue). The inset shows cyclic voltammogram of the irradiated solution at −80 °C. The estimated concentration of **tbMC** is 0.05 mM (using the average molar absorptivity obtained from repeated photoswitching measurements).

oxidation at 0.45 V supports its assignment to **tbMC**, and the generation of this merocyanine isomer via sequential oxidation and reduction of closed form **tbSP** as observed with cyclic voltammetry at higher scan rates (Figure 3).

UV−vis−NIR Spectroelectrochemistry. The UV−vis and NIR absorption spectrum of **tbMC**$^{+\bullet}$ at 1.0 V obtained spectroelectrochemically at room temperature shows strong absorption bands at 355 and 505 nm and weaker bands in the NIR region (777, 877, and 1008 nm, Figures 6 and S7). Subsequent reduction at 0.40 V resulted in a disappearance of the visible and NIR bands and the reappearance of the absorption band of **tbSP** at 310 nm together with a new absorption band at ca. 435 nm, assigned to *E*-**tbMCH**$^+$ (Figure S8). These assignments are consistent with time-dependent DFT (TD-DFT) calculations performed on these species and detailed in the Supporting Information. These changes contrast with those observed in the reversible one-electron oxidation of **MeNSP**, substituted with a nitro instead of tertbutyl groups, in which an absorption band at 457 nm of the radical cation of the closed form (i.e., **MeNSP**$^{+\bullet}$) appears and is relatively stable.[35] On the other hand, the NIR bands are comparable to

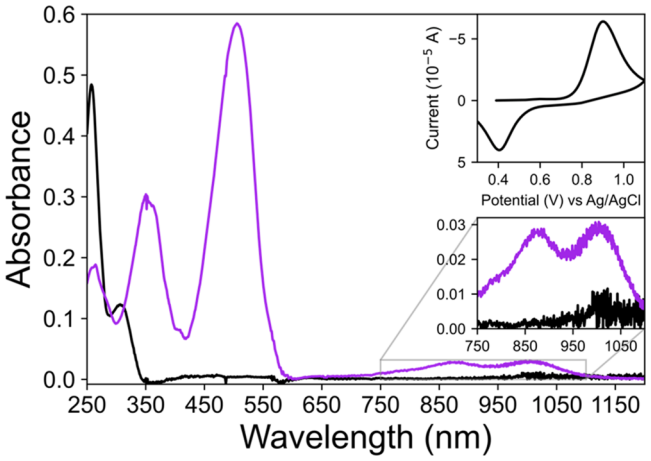

Figure 6. UV−vis and FT-NIR absorption spectra of **tbSP** (4 mM) in acetonitrile (0.1 M $TBAPF_6$) at room temperature before oxidation (black) and at 1.0 V generating **tbMC**$^{+\bullet}$ (violet). The inset shows the cyclic voltammogram at 0.01 V s^{-1}, and the NIR spectra are re-scaled to show progression of the 1008 nm band.

those observed for the radical cation of a spiropyran dimer,[35] but the respective visible absorption bands (443 and 478 nm) do not match those observed for **tbMC**$^{+\bullet}$ (355 and 505 nm). Furthermore, dimerization by indoline C−C coupling is not expected to occur upon oxidation of **tbSP** since the reactive para-carbon position of the indoline unit is blocked by a chloro substituent (Figure S9). Nevertheless, the absorption spectrum of **tbMC**$^{+\bullet}$ indicates that it is a similar type of radical cation with the radical delocalized over an extended conjugated system, and its reversible electrochemical generation shows that, at room temperature, **tbSP** essentially exhibits reversible switching of the oxidation state between the neutral closed form **tbSP** and the radical cation open form **tbMC**$^{+\bullet}$.

The thermally unstable species **tbSP**$^{+\bullet}$ and *E*-**tbMC** were generated as a demonstration of the full redox switching cycle by the preparative oxidation and reduction of **tbSP** at low temperature monitored by UV−vis absorption spectroscopy. At −80 °C, initially, a band at 466 nm appeared (Figure S10), after which it decreased in absorbance concomitant with an increase at 510 nm together with several NIR absorption bands (i.e., **tbMC**$^{+\bullet}$). Notably, the band at 466 nm corresponds to that of the closed form radical cation **MeNSP**$^{+\bullet}$;[35] thus, we assigned this absorption band to **tbSP**$^{+\bullet}$ (Figure S11). These data indicate that ring-opening in the oxidized state (from **tbSP**$^{+\bullet}$ to **tbMC**$^{+\bullet}$) occurs with a significant driving force and low barrier, consistent with the DFT results of Figure 4.

At a higher temperature (−60 °C), oxidation of **tbSP** resulted in the immediate appearance of the 466 nm band assigned to **tbSP**$^{+\bullet}$ as well as the characteristic absorption bands of **tbMC**$^{+\bullet}$ at 510 nm and several in the NIR (Figures 7 and S12). EPR spectroscopy at 77 K of this oxidized merocyanine species shows a single line at g = 2.004 and a linewidth of 1.2 mT, indicating significant broadening due to unresolved hyperfine coupling (Figure S13). In contrast, the EPR spectrum of the oxidized open form of the acridine spiropyran by Kubo et al. did exhibit hyperfine splitting.[38] This suggests that the radical in **tbMC**$^{+\bullet}$ is delocalized over an extensive part of the molecule including the indoline unit. The DFT-computed spin density supports this analysis (see the Supporting Information).

https://doi.org/10.1021/acs.jpca.1c01142
J. Phys. Chem. A 2021, 125, 3355−3361

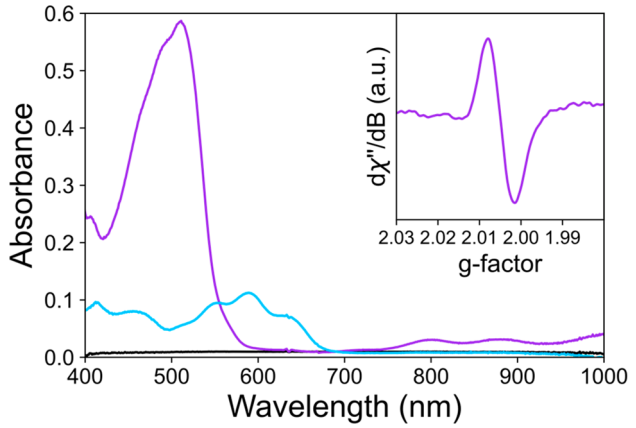

Figure 7. UV−vis absorption spectrum of **tbSP** (1 mM) in butyronitrile (0.1 M $TBAPF_6$) at −60 °C (black) after preparative oxidation to form **tbMC**$^{+\bullet}$ (violet) and after its subsequent reduction to **tbMC** (blue). The difference in applied potential for oxidation and that required for reduction was 1.2 V, consistent with cyclic voltammetry (Figure 3). The inset shows the EPR spectrum of **tbMC**$^{+\bullet}$ at 77 K.

Subsequent reduction at −60 °C resulted in the loss of absorbance from **tbMC**$^{+\bullet}$ and the appearance of a band at 590 nm with a vibrational progression characteristic of **tbMC**, which provides strong evidence of our proposed ring-opening of **tbSP** driven by a redox cycle, as well as an additional broad band at 455 nm assigned to the protonated species *E*-**tbMCH**$^+$ (Figures 7 and 8). It should be noted, however, that the data

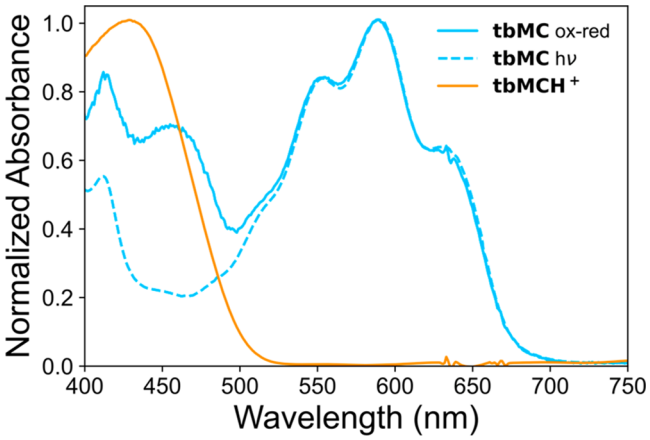

Figure 8. Normalized UV−vis absorption spectra of electrochemically generated **tbMC** (blue, solid), photochemically generated **tbMC** at −80 °C (blue, dashed), and a mixture of *Z*- and *E*-**tbMCH**$^+$ (orange) at PSS_{365} (prepared by protonation and irradiation of **tbSP**).

do not exclude formation of *Z*-**tbMC** also after reduction since this isomer will immediately ring-close to reform **tbSP**. The formation of the *E*-isomer through preparative oxidative and then reductive electrolysis indicates that *Z*−*E* isomerization is facile in the monocationic state (**tbMC**$^{+\bullet}$) with >25% yield. The yield is less than complete, partly due to the generation of protons at the working electrode "trapping" some of the *E*-**tbMC** in the thermally favored *E*-**tbMCH**$^+$ form (absorption band at 450 nm).[36,37] This effect limits the extent of oxidation that can be realized under the conditions employed. A second aspect to consider is the rapid equilibrium (low barriers) between **tbSP**$^{+\bullet}$ and **tbMC**$^{+\bullet}$, and hence, upon switching to a reducing potential, under diffusion-controlled conditions, the ring-closing to **tbSP**$^{+\bullet}$ followed by its subsequent reduction to **tbSP** competes with the desired reduction of **tbMC**$^{+\bullet}$ to *E*-**tbMC**. In the case of dithienylperhydrocyclopentene photochromes, this limit to efficiency was shown to be overcome when immobilized as monolayers on a surface[14] or incorporation in thin polymer films.[16]

CONCLUSIONS

The redox driven ring-opening of a photochromic spiropyran is facilitated by adding electron-donating tert-butyl substituents ortho- and para- to the phenolic oxygen of the benzopyran. The importance of the tert-butyl groups in achieving electrocatalytic ring-opening was evident in the work of Kubo et al. also,[38] and thus, we expect the formation of a thermodynamically stable phenoxy radical to drive the merocyanine formation. Additionally, next to preventing dimerization, the chloro substituent on the indoline unit is expected to destabilize the indoline-based radical cation that is formed initially also.

Although its redox potential is close to that of analogous (nitro-substituted) spiropyrans,[22] **tbSP** shows much less interference from protonation during electrochemical measurements, enabling ring-opening and *Z*−*E* isomerization of the zwitterion. Therefore, ring-opening and -closing of spiropyrans can be achieved by redox cycling in a manner analogous to the well-known photochemical pathway and with similar conversion efficiencies.

Ultimately, this approach to molecular switching opens up opportunities in controlling interfacial properties by transient electrochemical as well as photochemical stimuli and is especially of relevance to molecular-based devices in which optical access is limited.

ASSOCIATED CONTENT

Supporting Information

The Supporting Information is available free of charge at https://pubs.acs.org/doi/10.1021/acs.jpca.1c01142.

Supporting Information includes the synthetic procedure, additional spectroscopic and voltammetric data, and computational detail (PDF)

AUTHOR INFORMATION

Corresponding Authors

Denis Jacquemin − *Université de Nantes, CEISAM UMR 6230, CNRS, F-44000 Nantes, France;* orcid.org/0000-0002-4217-0708; Email: Denis.Jacquemin@univ-nantes.fr

Wesley R. Browne − *Molecular Inorganic Chemistry, Stratingh Institute for Chemistry, Faculty of Science and Engineering, University of Groningen, 9747 AG Groningen, The Netherlands;* orcid.org/0000-0001-5063-6961; Email: w.r.browne@rug.nl

Authors

Jorn D. Steen − *Molecular Inorganic Chemistry, Stratingh Institute for Chemistry, Faculty of Science and Engineering, University of Groningen, 9747 AG Groningen, The Netherlands*

Daniël R. Duijnstee − *Molecular Inorganic Chemistry, Stratingh Institute for Chemistry, Faculty of Science and Engineering, University of Groningen, 9747 AG Groningen, The Netherlands*

https://doi.org/10.1021/acs.jpca.1c01142
J. Phys. Chem. A 2021, 125, 3355−3361

Andy S. Sardjan − *Molecular Inorganic Chemistry, Stratingh Institute for Chemistry, Faculty of Science and Engineering, University of Groningen, 9747 AG Groningen, The Netherlands*

Jacopo Martinelli − *Molecular Inorganic Chemistry, Stratingh Institute for Chemistry, Faculty of Science and Engineering, University of Groningen, 9747 AG Groningen, The Netherlands*

Luuk Kortekaas − *Molecular Inorganic Chemistry, Stratingh Institute for Chemistry, Faculty of Science and Engineering, University of Groningen, 9747 AG Groningen, The Netherlands*

Complete contact information is available at: https://pubs.acs.org/10.1021/acs.jpca.1c01142

Author Contributions

The manuscript was written through contributions of all authors. All authors have given approval to the final version of the manuscript.

Notes

The authors declare no competing financial interest.

■ ACKNOWLEDGMENTS

Financial support was provided by The Netherlands Ministry of Education, Culture and Science (Gravity Program 024.001.035 to W.R.B.) This work used computational resources of the CCIPL center installed in Nantes.

■ REFERENCES

(1) Majima, T.; Tojo, S.; Ishida, A.; Takamuku, S. Cis − Trans Isomerization and Oxidation of Radical Cations of Stilbene Derivatives. *J. Org. Chem.* **1996**, *61*, 7793−7800.

(2) Spreitzer, H.; Scholz, M.; Gescheidt, G.; Daub, J. Electron-Transfer Chemistry and Redox-Switching of Stilbene-Like Heteroaromatic Compounds — Syntheses, Optoelectrochemical and ESR/ENDOR Studies. *Liebigs Ann.* **1996**, *1996*, 2069−2077.

(3) Yeh, L.-S. R.; Bard, A. J. The Electroreduction of Cis- and Trans-Thioindigo in N,N-Dimethylformamide Solutions. *J. Electroanal. Chem. Interfacial Electrochem.* **1976**, *70*, 157−169.

(4) Yeh, L.-S. R.; Bard, A. J. Electrochemical Studies and Photoconversion of Cis-and Trans-6,6′-Diethoxythioindigo. *J. Electroanal. Chem. Interfacial Electrochem.* **1977**, *81*, 333−338.

(5) Fox, M. A.; Hurst, J. R. Electrochemically Induced Pericyclic Reactions. A Radical Anionic Cyclization. *J. Am. Chem. Soc.* **1984**, *106*, 7626−7627.

(6) Neta, P.; Levanon, H. Spectrophotometric Study of the Radicals Produced by the Reduction of Syn- and Anti-Azobenzene. *J. Phys. Chem.* **1977**, *81*, 2288−2292.

(7) Goulet-Hanssens, A.; Utecht, M.; Mutruc, D.; Titov, E.; Schwarz, J.; Grubert, L.; Bléger, D.; Saalfrank, P.; Hecht, S. Electrocatalytic Z → E Isomerization of Azobenzenes. *J. Am. Chem. Soc.* **2017**, *139*, 335−341.

(8) Goulet-Hanssens, A.; Rietze, C.; Titov, E.; Abdullahu, L.; Grubert, L.; Saalfrank, P.; Hecht, S. Hole Catalysis as a General Mechanism for Efficient and Wavelength-Independent Z → E Azobenzene Isomerization. *Chem* **2018**, *4*, 1740−1755.

(9) Browne, W. R.; Pollard, M. M.; de Lange, B.; Meetsma, A.; Feringa, B. L. Reversible Three-State Switching of Luminescence: A New Twist to Electro- and Photochromic Behavior. *J. Am. Chem. Soc.* **2006**, *128*, 12412−12413.

(10) Logtenberg, H.; Areephong, J.; Bauer, J.; Meetsma, A.; Feringa, B. L.; Browne, W. R. Towards Redox-Driven Unidirectional Molecular Motion. *ChemPhysChem* **2016**, *17*, 1895−1901.

(11) Peters, A.; Branda, N. R. Electrochromism in Photochromic Dithienylcyclopentenes. *J. Am. Chem. Soc.* **2003**, *125*, 3404−3405.

(12) Peters, A.; Branda, N. R. Electrochemically Induced Ring-Closing of Photochromic 1,2-Dithienylcyclopentenes. *Chem. Commun.* **2003**, *8*, 954−955.

(13) Guirado, G.; Coudret, C.; Hliwa, M.; Launay, J.-P. Understanding Electrochromic Processes Initiated by Dithienylcyclopentene Cation-Radicals. *J. Phys. Chem. B* **2005**, *109*, 17445−17459.

(14) Areephong, J.; Browne, W. R.; Katsonis, N.; Feringa, B. L. Photo- and Electro-Chromism of Diarylethene Modified ITO Electrodes—towards Molecular Based Read−Write−Erase Information Storage. *Chem. Commun.* **2006**, *37*, 3930−3932.

(15) Browne, W. R.; Kudernac, T.; Katsonis, N.; Areephong, J.; Hjelm, J.; Feringa, B. L. Electro- and Photochemical Switching of Dithienylethene Self-Assembled Monolayers on Gold Electrodes. *J. Phys. Chem. C* **2008**, *112*, 1183−1190.

(16) Wesenhagen, P.; Areephong, J.; Fernandez Landaluce, T.; Heureux, N.; Katsonis, N.; Hjelm, J.; Rudolf, P.; Browne, W. R.; Feringa, B. L. Photochromism and Electrochemistry of a Dithienylcyclopentene Electroactive Polymer. *Langmuir* **2008**, *24*, 6334−6342.

(17) Nakashima, T.; Kajiki, Y.; Fukumoto, S.; Taguchi, M.; Nagao, S.; Hirota, S.; Kawai, T. Efficient Oxidative Cycloreversion Reaction of Photochromic Dithiazolylthiazole. *J. Am. Chem. Soc.* **2012**, *134*, 19877−19883.

(18) Kleinwächter, M.; Teichmann, E.; Grubert, L.; Herder, M.; Hecht, S. Oxidative and Reductive Cyclization in Stiff Dithienylethenes. *Beilstein J. Org. Chem.* **2018**, *14*, 2812−2821.

(19) Mutoh, K.; Nakano, E.; Abe, J. Spectroelectrochemistry of a Photochromic [2.2]Paracyclophane-Bridged Imidazole Dimer: Clarification of the Electrochemical Behavior of HABI. *J. Phys. Chem. A* **2012**, *116*, 6792−6797.

(20) Zhang, J.; Zou, Q.; Tian, H. Photochromic Materials: More Than Meets The Eye. *Adv. Mater.* **2013**, *25*, 378−399.

(21) Klajn, R. Spiropyran-Based Dynamic Materials. *Chem. Soc. Rev.* **2014**, *43*, 148−184.

(22) Kortekaas, L.; Browne, W. R. The Evolution of Spiropyran: Fundamentals and Progress of an Extraordinarily Versatile Photochrome. *Chem. Soc. Rev.* **2019**, *48*, 3406−3424.

(23) Nagashima, S.; Murata, M.; Nishihara, H. A Ferrocenylspiropyran That Functions as a Molecular Photomemory with Controllable Depth. *Angew. Chemie Int. Ed.* **2006**, *45*, 4298−4301.

(24) Mialane, P.; Zhang, G.; Mbomekalle, I. M.; Yu, P.; Compain, J.-D.; Dolbecq, A.; Marrot, J.; Sécheresse, F.; Keita, B.; Nadjo, L. Dual Photochromic/Electrochromic Compounds Based On Cationic Spiropyrans and Polyoxometalates. *Chem. - A Eur. J.* **2010**, *16*, 5572−5576.

(25) Saad, A.; Oms, O.; Marrot, J.; Dolbecq, A.; Hakouk, K.; El Bekkachi, H.; Jobic, S.; Deniard, P.; Dessapt, R.; Garrot, D.; et al. Design and Optical Investigations of a Spironaphthoxazine/Polyoxometalate/Spiropyran Triad. *J. Mater. Chem. C* **2014**, *2*, 4748−4758.

(26) Andrews, M. C.; Peng, P.; Rajput, A.; Cozzolino, A. F. Modulation of the Carboxamidine Redox Potential through Photoinduced Spiropyran or Fulgimide Isomerisation. *Photochem. Photobiol. Sci.* **2018**, *17*, 432−441.

(27) Preigh, M. J.; Stauffer, M. T.; Lin, F. T.; Weber, S. G. Anodic Oxidation Mechanism of a Spiropyran. *J. Chem. Soc. - Faraday Trans.* **1996**, *92*, 3991−3996.

(28) Wagner, K.; Byrne, R.; Zanoni, M.; Gambhir, S.; Dennany, L.; Breukers, R.; Higgins, M.; Wagner, P.; Diamond, D.; Wallace, G. G.; et al. A Multiswitchable Poly(Terthiophene) Bearing a Spiropyran Functionality: Understanding Photo- and Electrochemical Control. *J. Am. Chem. Soc.* **2011**, *133*, 5453−5462.

(29) Wagner, K.; Zanoni, M.; Elliott, A. B. S.; Wagner, P.; Byrne, R.; Florea, L. E.; Diamond, D.; Gordon, K. C.; Wallace, G. G.; Officer, D. L. A Merocyanine-Based Conductive Polymer. *J. Mater. Chem. C* **2013**, *1*, 3913−3916.

(30) Szalóki, G.; Alévêque, O.; Pozzo, J. L.; Hadji, R.; Levillain, E.; Sanguinet, L. Indolinooxazolidine: A Versatile Switchable Unit. *J. Phys. Chem. B* **2015**, *119*, 307−315.

(31) Hadji, R.; Szalóki, G.; Alévêque, O.; Levillain, E.; Sanguinet, L. The Stepwise Oxidation of Indolino[2,1-b]Oxazolidine Derivatives. *J. Electroanal. Chem.* **2015**, *749*, 1−9.
(32) Zhi, J. F.; Baba, R.; Hashimoto, K.; Fujishima, A. Photoelectrochromic Properties of a Spirobenzopyran Derivative. *J. Photochem. Photobiol., A* **1995**, *92*, 91−97.
(33) Jukes, R. T. F.; Bozic, B.; Hartl, F.; Belser, P.; De Cola, L. Synthesis, Photophysical, Photochemical, and Redox Properties of Nitrospiropyrans Substituted with Ru or Os Tris(Bipyridine) Complexes. *Inorg. Chem.* **2006**, *45*, 8326−8341.
(34) Natali, M.; Giordani, S. Interaction Studies between Photochromic Spiropyrans and Transition Metal Cations: The Curious Case of Copper. *Org. Biomol. Chem.* **2012**, *10*, 1162−1171.
(35) Ivashenko, O.; van Herpt, J. T.; Rudolf, P.; Feringa, B. L.; Browne, W. R. Oxidative Electrochemical Aryl C−C Coupling of Spiropyrans. *Chem. Commun.* **2013**, *49*, 6737−6739.
(36) Mendive-Tapia, D.; Kortekaas, L.; Steen, J. D.; Perrier, A.; Lasorne, B.; Browne, W. R.; Jacquemin, D. Accidental Degeneracy in the Spiropyran Radical Cation: Charge Transfer between Two Orthogonal Rings Inducing Ultra-Efficient Reactivity. *Phys. Chem. Chem. Phys.* **2016**, *18*, 31244−31253.
(37) Kortekaas, L.; Chen, J.; Jacquemin, D.; Browne, W. R. Proton-Stabilized Photochemically Reversible E/ Z Isomerization of Spiropyrans. *J. Phys. Chem. B* **2018**, *122*, 6423−6430.
(38) Hirao, Y.; Taniguchi, T.; Teraoka, M.; Kubo, T. Redox/PH Dual Stimuli-Responsive Acridine Spiropyran. *Asian J. Org. Chem.* **2019**, *8*, 863−866.
(39) Stoll, S.; Schweiger, A. EasySpin, a comprehensive software package for spectral simulation and analysis in EPR. *J. Magn. Reson.* **2006**, *178*, 42−55.
(40) Fischer, E.; Hirshberg, Y. Formation of Coloured Forms of Spirans by Low-Temperature Irradiation. *J. Chem. Soc.* **1952**, 4522−4524.

https://doi.org/10.1021/acs.jpca.1c01142
J. Phys. Chem. A 2021, 125, 3355−3361